Journal of the Nigerian Association of Mathematical Physics
Volume **22 (November, 2012), pp 85 – 94**

Radiative Forcing of Urban Aerosols in the Near Infrared Region

B. I. Tijjani

Department of Physics, Bayero University, Kano

Abstract

We study the radiative forcing of Urban aerosols at the near infrared region $(1.0\ \mu m\ to\ 4.0\ \mu m)$ ***using data from the Optical Properties of Aerosol and Clouds software. Radiative forcing at different wavelengths and Relative humidities (RHs) are calculated and analysed. The other parameters that were analysed in order to be able to understand the nature of the particles and their distributions are the effective refractive indicies, optical depths, single scattering albedo, extinction, scattering and absorption coefficients. From the analysis, it was discovered that radiative forcing (in a form of cooling) increases with relative humidities (RH) and is dependent on wavelengths. The nature of the increments of the radiative forcing with RH reflects the dominance of fine particles. This is because as a result of the increase in RH from 0 to 50%, large particles started sedimenting which caused the increase in fine particles. As the RH increases the concentrations of larger particles continue to decrease so the concentration of fine particles continue to increase which result in decrease in effective radii and increase in Angstrom coefficients. The analysis of the Angstrom coefficients showed the dominance of fine particles. The analysis of optical depth with wavelengths and RHs together with the comparison with scattering and absorption coefficients, hygsroscopicity factor and humidification factor, show that the particles are very hygroscopic and have bimodal type of size distributions with majority satisfying Junge type of distribution with a small component of lognormal.***

1.0 Introduction

It is generally clear that aerosols perturb the radiation balance of the Earth both directly, by scattering and absorbing solar radiation, and indirectly by changing the microphysical properties of the clouds [[1-4].

Great progress has been made in recent years in the use of satellite sensors for the quantitative characterization of aerosol optical properties [5,6]. Aerosol optical thickness and aerosol effective radius (r_{eff}) are two commonly retrieved properties. There has recently been an increase in the use of satellite derived aerosol products for the study of urban particulate (PM) [7-9]. The ultraviolet, visible, near-infrared and infrared spectral regions are increasingly being exploited for the remote sounding of the Earth's atmosphere and surface [10].

The absorption of water by atmospheric aerosols with increasing relative humidity (RH) influences their size, composition, lifetime, chemical reactivity, and light extinction, scattering and absorption. Water is the most prevalent aerosol component at RHs above 80% and is often a significant component at lower RHs [11]. Accordingly, hygroscopic growth is important in a number of air pollution problems, including visibility impairment, climate effects of aerosols, acid deposition, long-range transport, and the ability of particles to penetrate into the human respiratory system.

The aerosol properties needed to estimate the magnitude and sign of direct aerosol radiative forcing are the aerosol optical depth, τ (integral of aerosol extinction with height), single scattering albedo, ω (ratio of the aerosol scattering coefficient to total extinction coefficient), and the aerosol up scatter fraction, β (fraction of radiation scattered upward to space) [12-14] Analysis of optical depths at different spectral wavelengths helps in deriving information on the optical properties and size distribution of particles, as well as studying the diurnal and season variability of aerosols [15].

The aim of this paper is to calculate and analyze the spectral variation of Radiative forcing with relative humidities (0, 50, 70, 80, 90, 95, 98 and 99%) for urban aerosols at the near-infrared region from the data extracted from OPAC. The spectral variations of optical depths, absorption, scattering and extinction coefficients are analysed to determine the particles size distributions and the effect of hygroscopic growth as a result of increase in RH with the change in mode size distributions.

Corresponding author-, E-mail: idrith@yahoo.com, idrihtijjani@gmail.com, Tel. +234 8037030877

2.0 Methodology

The data used for the urban aerosols in this paper are derived from the Optical Properties of Aerosols and Clouds (OPAC) data set [16]. In this, a mixture of three components is used to describe Urban aerosols: a water soluble components (WASO, consists of scattering aerosols, that are hygroscopic in nature, such as sulfates and nitrates present in anthropogenic pollution), water insoluble (INSO) and soot (SOOT, not soluble in water and therefore the particles are assumed not to grow with increasing relative humidity).

The globally averaged direct aerosol Radiative forcing, ΔF_R, was calculated using the equation derived by [17]

$$\Delta F_R = -\frac{S_0}{4} T_{atm}^2 (1-N)\{(1-A)^2 2\beta\tau_{sca} - 4A\tau_{abs}\} \quad (1)$$

Where S_0 is a solar constant, T_{atm} is the transmittance of the atmosphere above the aerosol layer, N is the fraction of the sky covered by clouds, A is the albedo of underlying surface, β is the fraction of radiation scattered by aerosol into the atmosphere and τ_{sca} and τ_{abs} are the aerosol layer scattering and absorption of orptical thickness respectively. The above expression gives the radiative forcing due to the change of reflectance of the earth-aerosol system. The upscattering fraction is calculated using an approximate relation [18]

$$\beta = \frac{(1-g/2)}{2} \quad (2)$$

The global averaged albedo A=0.22 over land and A=0.06 over the ocean with 80% of aerosols being over the land; solar constant of 1370Wm^{-2}, the atmospheric transmittance is taken to be Tatm=0.79 [19] and cloudness N=0.6.

To determine the relationship between wavelengths and effective refractive indices the following formula is used for the four mixed aerosols [20]:

$$\frac{\varepsilon_{eff}-\varepsilon_0}{\varepsilon_{eff}+2\varepsilon_0} = \sum_{i=1}^{3} f_i \frac{\varepsilon_i-\varepsilon_0}{\varepsilon_i+2\varepsilon_0} \quad (3)$$

where f_i and ε_i are the volume fraction and dielectric constant of the ith component and ε_0 is the dielectric constant of the host material. For the case of Lorentz-Lorentz [21,22], the host material is taken to be vacuum, ε_0 =1.

The spectral behavior of the aerosol optical thickness, scattering, absorption, and extinction coeffecients can be used to obtain some information regarding the size distribution by just looking at the Angstron coefficient exponent that expresses the spectral dependence of aerosol optical depth ($\tau(\lambda)$), scattering ($\sigma_{scat}(\lambda)$), absorption ($\sigma_{abs}(\lambda)$) and extinction ($\sigma_{ext}(\lambda)$) coefficients, with the wavelength of light (λ) as inverse power law [23,24]:

$$X(\lambda)=\beta\lambda^{-\alpha} \quad (4)$$

Where X(λ) can be any of the parameters mentioned above. In this paper optical depths ($\tau(\lambda)$)are used but other paramenters are used for comparisons. The formula is derived on the premise that the extinction of solar radiation by aerosols is a continuous function of wavelength, without selective bands or lines for scattering or absorption [25].

The wavelength dependence of τ(λ) can be characterized by the Angstron parameter, which is a coefficient of the following regression:

$$\ln\tau(\lambda) = -\alpha\ln(\lambda) + \ln\beta \quad (5)$$

where β and α are the turbidity coefficient and the shaping factor, respectively [26,27]. The turbidity coefficient is a proportionality constant relating the optical depth and the wavelength. The shaping factor α provides a measure of how rapidly aerosol optical depth τ changes with wavelength and also relates to the size of particles and depends on the ratio of the concentration of large to small aerosols and β represents the total aerosol loading in the atmosphere. So α and β can be used to describe the size distribution of aerosol particles and the general haziness of the atmosphere. Larger particles generally correspond to smaller α, whereas smaller particles generally correspond to larger α. According to [28], 2000 a low (down to 0) is a sign of large dust particles; a high (up to 2) corresponds to small smoke particles. Also according to [29] typical values of the shaping factor are larger than 2.0 for fresh smoke particles and close to zero for Sahelian Saharan dust particles. The dust studies seem to yield shaping factors in the range of approximately 0.2, whereas particles produced from biomass burnings yielded shaping factors around 1.5 and higher. Large positive values of α are characteristic of fine-mode-dominated aerosol size distributions [25,29,30] while near zero and negative values are characteristic of dominant coarse-mode or bi-modal size distributions, with coarse-mode aerosols having significant magnitude [29,31,32].

In the analysis of spectral measurement of optical depths in locations dominated by biomass burning, urban, or desert dust aerosols, a significant curvature in the ln τ versus ln λ relationship was observed [29]. In this paper, an attempt has been made to show the departure that introduces a curvature on lnτ(λ) versus lnλ curve. And a second order fit to the lnτ(λ) versus lnλ provides better estimates than linear fit [32-34]. The quadratic formula that is used is

$$\ln\tau(\lambda) = -\alpha_2(\ln\lambda)^2 - \alpha_1\ln\lambda + \ln\beta \quad (6)$$

and the coefficients (β, α_1, α_2) are obtained using SPSS 15 for windows. In case of negative curvature (α_2<0, convex type curves) the rate of change of α is more significant at the longer wavelengths, while in case of positive curvature (α_2 >0, concave type curves) the rate of change of α is more significant at the shorter wavelengths. [29] reported the existence of negative curvatures for fine-mode aerosols and positive curvatures for significant contribution by coarse-mode particles in the size distribution.

To quantify the water uptake at subsaturated conditions, we define the hygroscopic growth factor (HGF) as the ratio of the radius R_{RH}, radius at a specified RH to the original dry radius R_{dry}, which is at RH=0% [35,36]:

$$HGF = \frac{R_{RH}}{R_{dry}} \quad (7)$$

The HGF can be subdivided into different classes with respect hygroscopicity. One classification is based on diameter growth factor by [35,37] as Barely Hygroscopic (BH; HGF = 1.0–1.11), Less Hygroscopic (LH; HGF = 1.11–1.33), More Hygroscopic (MH; HGF = 1.33–1.85) .

In order to obtain a better estimate and be able to explain the type of direct climate forcing by aerosols and reduce the associated uncertainty, quantification of aerosol optical properties and their dependency on relative humidity [38-40] is very important. The increase in light-scattering, absorption and extinction coefficients by aerosols with RH with respect to wavelength, f(RH, λ), (humidification factor), has been considered an important parameter to describe the nature of aerosol Radiative forcing [3,39,41-46] and to understand the cause of visibility degradation due to aerosols [47-49]. The humidification factor of aerosols influences the particle size distribution and refractive indices and hence, several key optical properties of aerosols (e.g., scattering, extinction and absorption coefficients, single scattering albedo, asymmetry parameter, and aerosol optical depth) that are relevant to aerosol radiative forcing estimates [38-40].

The aerosol humidification factor, f(RH, λ), can be described as either the ratio of aerosol light scattering, absorption, or extinction between two different RH values. The f(RH, λ) was calculated from the following [50]:

$$f(RH,\lambda) = \frac{\sigma_{ext}(RH_{high},\lambda)}{\sigma_{ext}(RH_{ref},\lambda)} = \left(\frac{100-RH_{ref}}{100-RH_{high}}\right)^{\gamma} \quad (8)$$

where in this study RH_{ref} is 0%, γ is referred to as the aerosol hygroscopicity factor. Hygroscopic properties of aerosol particles describe the interactions between particles and the surrounding water vapor including the critical size needed to activate the growth of a particle into a cloud droplet by water vapor condensation in given conditions. The γ parameter in our case was obtained by combining the eight $\sigma_{ext}(\lambda)$ values at 0%, 50%, 70%, 80%, 90%, 95%, 98% and 99% RH. The use of γ has the advantage of describing the hygroscopic behavior of aerosols in a linear manner over a broad range of RH values; it also implies that particles are deliquesced [52]., 2005). The γ parameter is dimensionless, and it increases with increasing particle water uptake. From previous studies, typical values of γ for ambient aerosol ranged between 0.1 and 1.5 [51-53].

3.0 Results and Discussions

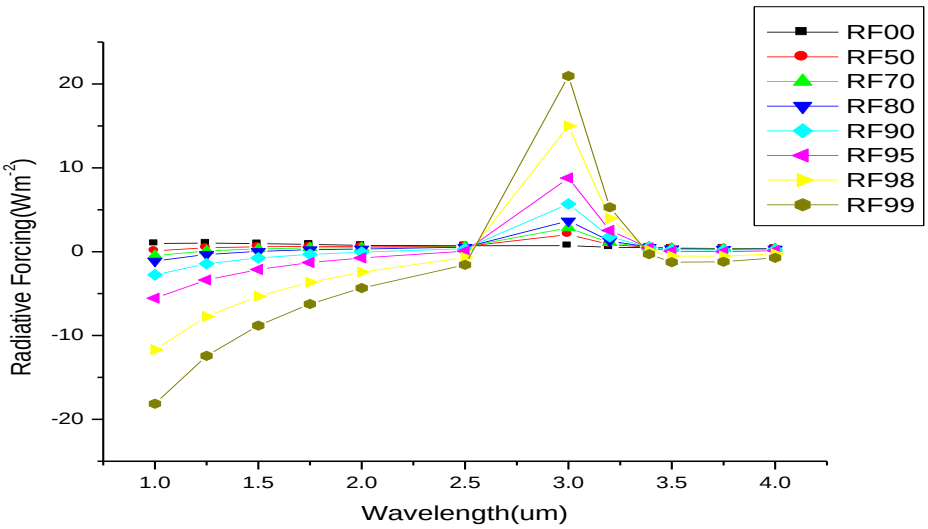

Figure 1: A plot of radiative forcing against wavelength

From figure 1, at 0% RH the RF is positive and almost independent of wavelength. But as the RH increases the RF continues to decrease most especially at shorter wavelengths and this indicates the dominance of fine mode particles because they scatter more light as a result of hygroscopic growth than coarse particles which results in the increase in cooling at 1.0 to 2.5 spectral range . But as from 2.5 to 3.0 there is a sudden change in RF which indicates the sudden change in size distribution from Junge size distribution of fine mode particles to a small lognormal size distribution of coarse mode particles that don't vary much with the increase in RH. The relation of RF with RH is such that at the deliquescence point (90 to 99%) the increase or decrease with higher humidities increases or decreases substantially, making this process strongly nonlinear with relative humidity [54,55].

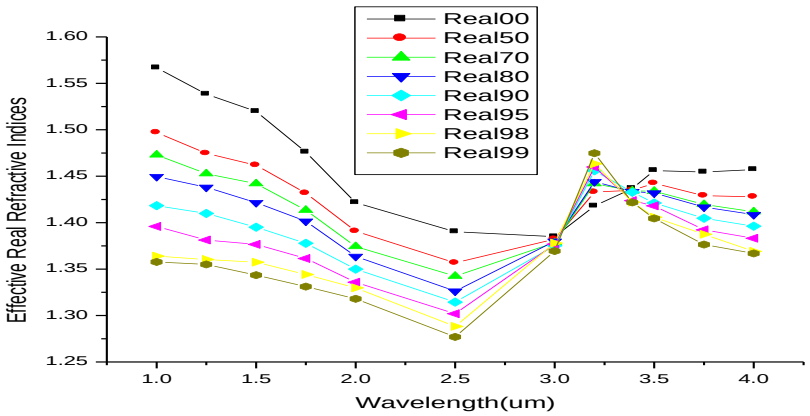

Figure 2: A graph of effective real refractive indices against wavelengths

The decrease in the effective real refractive indicies with RH is as a result of hygroscopic growth. The relationship of the particles with wavelengths shows the presence of non-spherical particles.

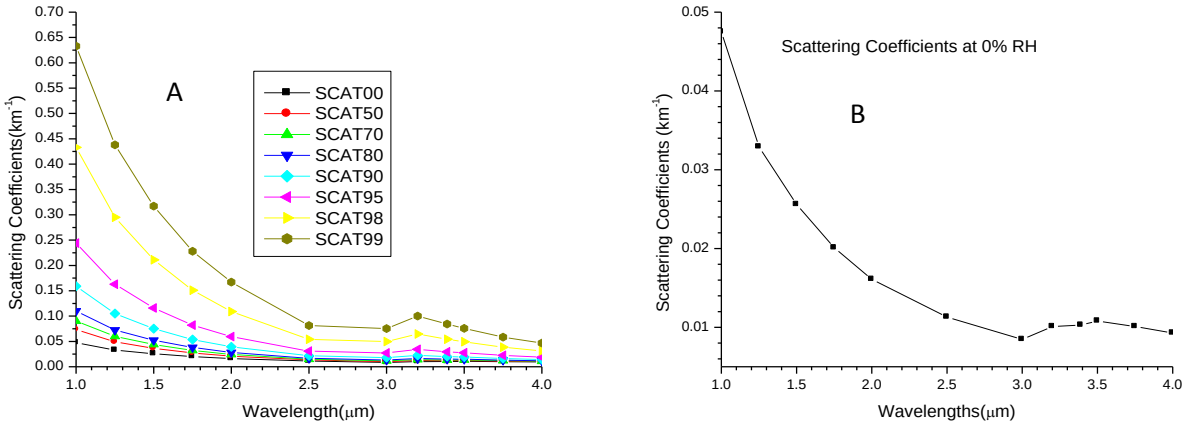

Figure 3: A plot of scattering coefficients against wavelength (A) for relative humidities 0% to 99% (B) for 0% Relative humidity.

Figure 3B is drawn to enable us see more clearly the type of relationship between scattering coefficient and wavelength. Comparing figures 3A and 3B it can be observed that scattering coefficient has bimodal type of size distributions. The first at the spectral range 1.0μm to 3.0μm which indicates that power law is satisfied (ie it can be approximated with a power law wavelength dependence equations (4) and (5)) while the second (3.0μm to 4.0μm) is a lognormal mode. The increase in scattering coefficients with RH is as a result of hygroscopic growth by the aerosols particles where by fine particles scatter more light than coarse particles.

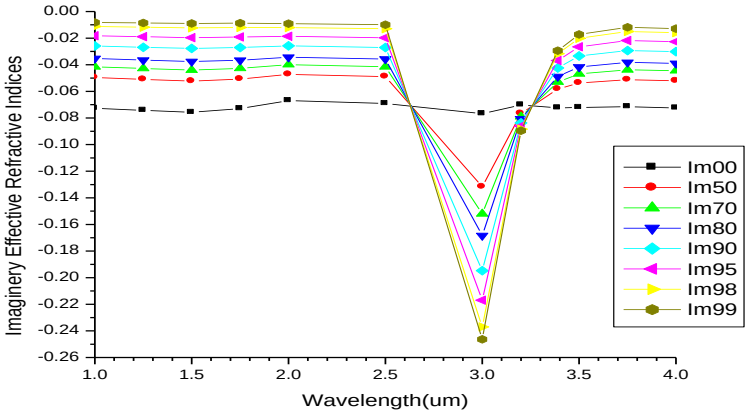

Figure 4: A plot of effective imaginary refractive indices against wavelengths

From figure 4 at RH=0% it shows little variations of the effective refractive indicies with wavelength which shows the presence of non-spherical particles. But as the RH increases there is a decrease in the indicies and a creation of two types of mode size distributions a the atmospheric window of 3.0μm.

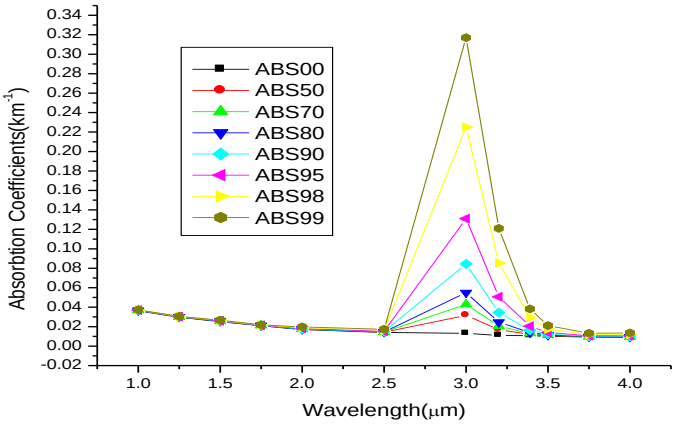

Figure 5: A graph of absorption against wavelengths

It decreases slowly with wavelength and independent of RH, in the interval 1.0μm to 2.5μm.
It shows the presence of two distinct size distribution that satisfy Junge power law (1.0μm to 2.5μm.) and lognormal (2.5μm to 4.0μm.) modes. The first spectral is independent of RH and this reflects the dominance of fine particles but the second is dependent on RH and this reflects the dominance of coarse mode particles.

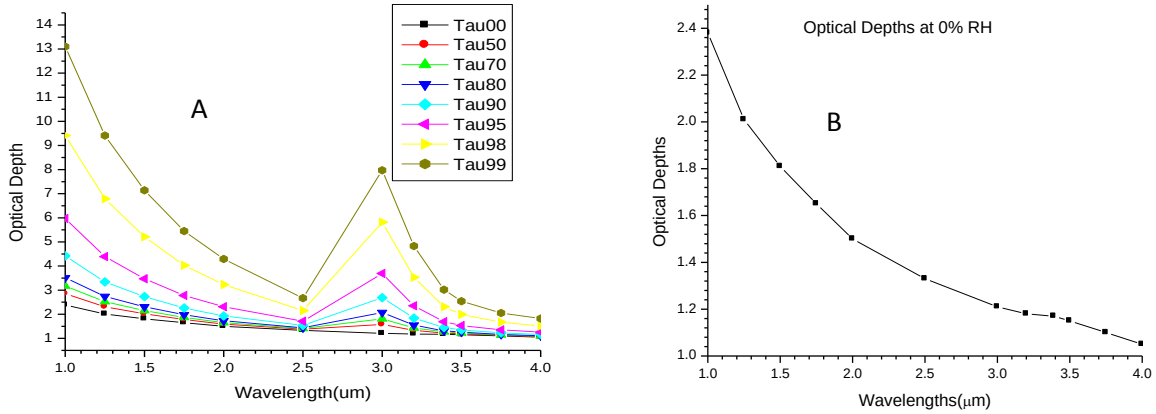

Figure 6: A plot of optical depth against wavelengths (A) for relative humidities 0 % to 99% (B) for 0% relative humidity.

Figure 6B is drawn to enable us see more clearly the type of relationship between optical depth and wavelength. At 0% RH (figure 6B) it appears the system has bimodal of the form Junge (1.0μm to 3.0μm) and lognormal (3.0μm to 4.0μm). But as the RH increases, the bimodal type of distribution becomes clearer, but this time at 1.0μm to 2.5μm (Junge) and a small lognormal (2.5μm to 4.0μm). It is evident from the figure that there is relatively strong wavelength dependence of optical depth at shorter wavelengths that gradually decreases towards longer wavelengths at two spectral interval (1.0 to 2.5 and 3.0 to 4.0) irrespective of the RH change, attributing to the presence of fine and coarse particles at these two different size modes distributions respectively. The first mode which is dominated by fine mode particles satisfies power law distribution while the second dominated by coarse mode satisfy lognormal size distribution. This is in line with what [56] determined that the majority of aerosol size distributions could best be represented by a two-component size distribution consisting of a Junge-type distribution plus a small component of larger particles of lognormal type. The high optical depth is linked to a hygroscopic and/or coagulation growth from the fine aerosols. Furthermore, the fine mode aerosols have hydrate and coagulated characters that become large particles, causing the AOD to increase

Table 1: The results of the Angstron coefficients at the respective relative humidities using equation(5) at the spectral range 1.0μm to 2.5μm.

	Linear			Quadratic			
RH	α	β	R^2	α_1	α_2	β	R^2
0	0.6308	2.3453	0.9969	0.7208	-0.0989	2.3725	0.9989
50	0.7969	2.7987	0.9964	0.9338	-0.1505	2.8481	0.9994
70	0.8879	3.1036	0.9968	1.0336	-0.1601	3.1619	0.9995
80	0.9763	3.4481	0.9975	1.1172	-0.1549	3.5108	0.9999
90	1.1575	4.3645	0.9990	1.2586	-0.1111	4.4212	0.9997
95	1.3640	5.9734	0.9999	1.3521	0.0130	5.9643	0.9999
98	1.6031	9.6936	0.9974	1.3500	0.2782	9.3849	0.99997
99	1.7160	13.7141	0.9934	1.2821	0.4769	12.9741	0.9999

The observed variations in Ångström coefficients can be explained by changes in the effective radius of a mixture resulting from changes in RH: the larger the number of small aerosol particles, the smaller the effective radius and the larger the Ångström coefficient. This shows that hygroscopic growth has caused reduction in the effective radii and this is caused α to increase with the increase in RH. It also shows that increase in RH which increases hygroscopic growth has caused increase in mode size distributions for the two modes. Though [29] reported the existence of negative curvatures for fine-mode aerosols and positive curvatures for significant contribution by coarse-mode particles in the size distribution but from table 1, it can be observed that RH also has effect on the type of curvature. This is because from 0 to 90% RH $\alpha_2<0$ which signifies fine particles while at RH 95 to 99% RH $\alpha_2>0$ for coarse particles.

Table 2: Values of dry and wet radii of aerosols extracted from the microphysical characteristics of the aerosols and the calculated HGF using equation(7).

RH(%)	00	50	70	80	90	95	98	99
Rmod (wet), [um]:	0.0212	0.0262	0.0285	0.0306	0.0348	0.0399	0.0476	0.0534
Rmod (dry), [um]:	0.0212	0.0212	0.0212	0.0212	0.0212	0.0212	0.0212	0.0212
HGF	1	1.236	1.344	1.443	1.642	1.882	2.245	2.519
MAS.MIXof WASO(%)	46.41	56.32	60.85	64.75	71.52	78.22	85.35	88.98

Table 2 shows that the mixture is very hygroscopic.

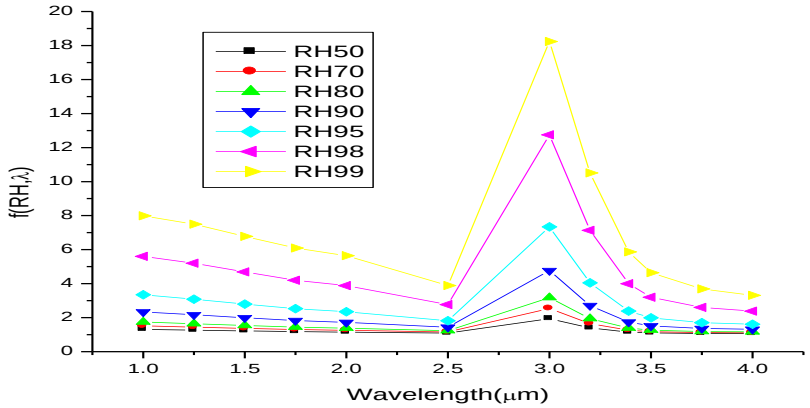

Figure 7: A graph of f(RH, λ) against wavelengths

It relation with RH shows that the mixture is very hygroscopic. This is not surprising because it contains large amount of water soluble component. It also shows increase in mode size distributions as a result of increase in RH. The figure shows bi-modal types of size distribution (Junge (1.0μm to 2.5 μm) and lognormal (2.5 μm to 4.0 μm)). It also shows the sensitivity of the sudden change in size distribution at 3.0 atmospheric window.

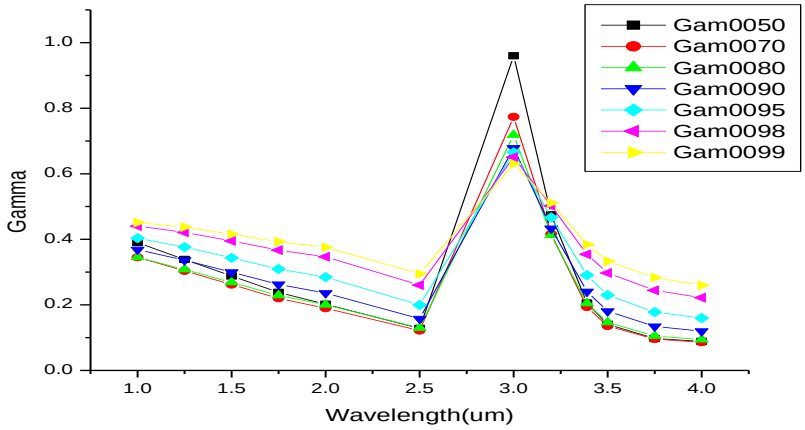

Figure 8: A graph of hygroscopicity factor against wavelengths

The figure shows that the particles are deliquesced as cited by [52]. This is in line with the previous studies by [51-53] that typical values of γ for ambient aerosol ranged between 0.1 and 1.5.

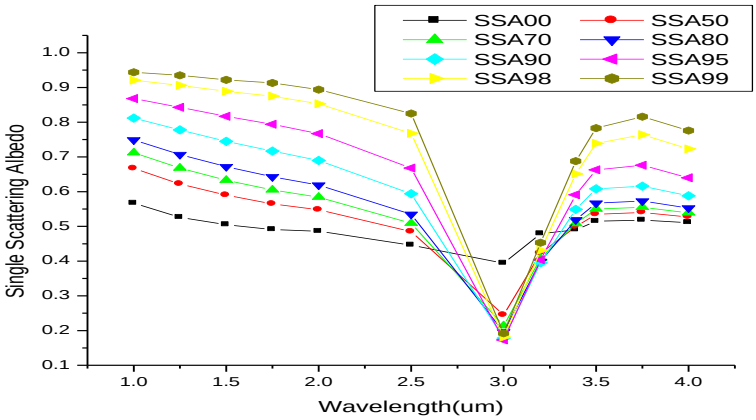

Figure 9: A plot of single scattering albedo against wavelengths

The decrease in SSA with wavelengths signifies the dominance of fine modes particles. This is because as discussed before fine mode particles scatter more lights at shorter wavelengths. Its relation with RH also confirms that fine more particles scatter more lights as a result of the increase in hygroscopic growth. Its behavior at 3.0μm atmospheric window shows its sensitivity to particle size distributions with wavelengths and RH.

5.0 Conclusion

The nature of the increments of the radiative forcing with RH reflects the dominance of fine particles at spectral range of 1.0 μm to 2.5 μm and the dominance of coarse particles at 2.5 μm to 4.0 μm.

This is because as a result of increase in RH fine particles are effected with hygroscopic growth which scatter more lights thereby increasing cooling while coarse are not very sensitive. The increase in Angstrom coefficient with RH shows that as the RH increase the coarse particles continue sediment which caused the increase in the concentration of fine particles which result in decrease in effective radius and increase in Angstrom coefficients. The analysis of optical depth with wavelengths together with the comparison with scattering and absorption coefficients, hygsroscopicity factor and humidification factor show that the particles have bimodal type of size distributions with majority satisfying Junge type of distribution with a small component of lognormal.

Reference

[1] Waggoner, A. P., Weiss R. E., Ahlquist N. C., Covert D. S., Will S., and Charlson R. J.(1981) Optical characteristics of atmospheric aerosols, Atmos. Environ., 15, 1891– 1909,.

[2] Albrecht, B. A., (1989)Aerosols, cloud microphysics, and fractional cloudiness, Science Reports, 245, 1227– 1230,.

[3] Charlson, R.J., Schwartz, S.E., Hales, J.M., Cess, R.D., Coakley, J.A., Hansen, J.E. and Hoffmann, D.J. (1992). Climate Forcing by Anthropogenic Aerosols. Science. 255: 423-430.

[4] Schwartz, S. E.(1996) The whitehouse effect-shortwave radiative forcing of climate by anthropogenic aerosols: an overview, J. Aerosol Sci., 3, 359– 382,.

[5] King, M.D., Kaufman Y.J., Tanre D., and Nakajima T., (1999) Remote sensing of tropospheric aerosols from space: past, present, and future, *Bull. Amer. Meteor. Soc., 80*, 2229-2259,

[6] Kaufman, Y.J., Tanre D., and Boucher O., (2002) A satellite view of aerosols in climate systems, *Nature, 419*, 215-223.

[7] Wang, J. & Christopher, A. (2003). Inter-comparison between satellite-derived aerosol optical thickness and PM2.5 mass: Implications for air quality studies. Geophysics Research Letters, Vol. 30, 1-4.

[8] Chu, D.A., Kaufman, Y.J., Zibordi, G., Chern, J.D., Mao, J., Li, C. & Holben, B.N. (2003). Global monitoring of air pollution over land from the Earth Observing System-Terra Moderate Resolution Imaging Spectroradiometer (MODIS). Journal of Geophysical Research, Vol 108, 4661.

[9] Engle-Cox, J. A., Holloman, C.H. & Coutant, B. W. (2004). Qualitative and quantitative evaluation of MODIS satellite sensor data for regional and urban scale air quality. Atmospheric Environment , 38, 2495-2509.

[10] Buchwitz M., Rozanov V. V. and Burrows J. P. (2000) A correlated-k distribution scheme for overlapping gasses suitable for retrieval of atmospheric constituents from moderate resolution radiance measurements in the visible/near-infrared spectral region, ;Journal of Geophysical Research Vol.105, No. D12, p15247-15261

[11] Hanel, G. (1976). The Properties of Atmospheric Aerosol Particles as Functions of Relative Humidity at Thermodynamic Equilibrium with Surrounding Moist Air. In *Advances in Geophysics, Vol. 19*,H. E. Landsberg and J.Van Mieghem, eds., Academic Press, New York, pp. 73–188.

[12] Chylek, P., and J. A. Coakley, (1975) Man-made aerosols and the heating of the atmosphere over polar regions, in Climate of the Arctic: Twenty-Fourth Alaska Science Conference, Fairbanks, Alaska, August 15 to 17, , edited by G. Weller and S. A. Bowling, pp. 159–165, Geophysical Institute, Univ. of Alaska, Fairbanks, 1975.

[13] Haywood, J. M., and Shine K. P.,(1995) The effect of anthropogenic sulfate and soot aerosol on the clear sky planetary radiation budget, Geophys. Res. Lett., 22, 603–606.

[14] Russell, P. B., Kinne S. A., and Bergstrom R. W.(1997) Aerosol climate effects: Local radiative forcing and column closure experiments, J. Geophys. Res., 102, 9397–9407.

[15] Rana S., Kant Y., Dadhwal V.K (2009), *Diurnal and Seasonal Variation of Spectral Properties of Aerosols over Dehradun, India* Aerosol and Air Quality Research, Vol. 9, No. 1, pp. 32-49, 2009

[16] Hess M., Koepke P., and Schult I (May 1998), Optical Properties of Aerosols and Clouds: The Software Package OPAC, Bulletin of the A merican Met. Soc. **79**, 5, p831-844.

[17] Chylek, P., and Wong J. (1995), Effect of absorbing aerosols on global radiation budget, Geophys . Res. Lett., 22(8), 929–931, doi: 10.1029/95GL00800.

[18] Segan, C. and Pollack J.(1967) Anisotropic nonconservative scattering and the clouds of Venus, J. Geophys. Res., 72, 469-477.

[19] Penner, J. E. Dickinson R.E. and O'Neil C. A. (1992) Effects of aerosols form biomass on the global radiation budget, Science, 256, 1432-1434.

[20] Aspens D. E. (1982), Local-field effect and effective medium theory: A microscopic perspective Am. J. Phys. 50, 704-709.

[21] Lorentz, H. A. (1880). Ueber die Beziehung zwischen der Fortpflanzungsgeschwindigkeit des Lichtes und der Korperdichte. Ann. Phys. Chem. 9, 641–665.

[22] Lorenz, L. (1880). Ueber die Refractionconstante. A nn. P hys. Chem. 11, 70–103.

[23] Angstrom, A., (1929): On the atmospheric transmission of sun radiation and on dust in the air. Geogr. Ann., 11, 156-166.

[24] Ångström, A.K. (1961). Techniques of Determining the Turbidity of the Atmosphere. Tellus XIII: 214.

[25] Ranjan, R.R., Joshi, H.P. and Iyer, K.N. (2007). Spectral variation of total column aerosol optical depth over Rajkot: A tropical semi-arid Indian station. Aerosol Air Qual. Res. 7: 33-45.

[26] Liou K. N.,(2002) An Introduction to Atmospheric Radiation, 2nd ed. Academic, San Diego, Calif.,.

[27] O'Neill N. T., and Royer A. (1993) Extraction of binomial aerosol-size distribution radii from spectral and angular slope (Angstrom) coefficients, Appl. Opt. 32, 1642-1645.

[28] Dubovik, O., et. al., (2000): Accuracy assessments of aerosol optical properties retrieved from Aerosol Robotic Network (AERONET) Sun and sky radiance measurments, JGR, 105, 9791 - 9806.

[29] Eck, T.F., B.N.Holben, J.S.Reid, O.Dubovik, A.Smirnov, N.T.O'Neill, I.Slutsker, and S.Kinne, (1999), The wavelength dependence of the optical depth of biomass burning, urban and desert dust aerosols, J.Geoph.Res., 104, 31,333-31,350,.

[30] Eck, T. F., et al. (2005), Columnar aerosol optical properties at AERONET sites i n cen tr al easte rn Asia a nd aer osol tr anspor t t o t he tropic al mid -Pacific, J. Geophys. Res. , 110 , D06202, doi:10.1029/2004JD005274

[31] O'Neill, N.T., Dubovic, O. and Eck, T.F. (2001). Modified Angstrom Exponent for the Characterization of Submicrometer Aerosols. Appl. Opt. 40: 2368-2375.

[32] Kaskaoutis, D.G. and Kambezidis, H.D. (2006). Investigation on Wavelength Dependence of the Aerosol Optical Depth in the Athens Area. Q.J.R Meteorol. Soc. 132: 2217-2234.

[33] Eck, T. F., B. N. Holben, O. Dubovic, A. Smirnov, I. Slutsker, J. M. Lobert, and V. Ramanathan (2001), Column-Integrated aerosol optical properties over the Maldives during the northeast monsoon for 1998-2000 (2001), J. Geophys. Res., 106, D22, 28555-28566.

[34] Kaskaoutis, D. G., and H. D. Kambezidis, A. D. Adampoulos, and P. A. Kassomenos (2006), On the characterization of aerosols using the Ångström exponent in the Athens area, J. Atmos. Solar-Terr. Phys., 68, 2147-2163.

[35] Swietlicki, E.,et. al. (2008) Hygroscopic properties of submicrometer atmospheric aerosol particles mea-sured with H TDMA instruments in various environments–A review, Tellus B, 60, 432–469,.

[36] Randles , C. A. , Russell L. M. and. Ramaswamy V. (2004) Hygroscopic and optical properties of organic sea salt aerosol and consequences for climate forcing, Geophys. Res. Lett., 31, L16108, doi:10.1029/2004GL020628.

[37] Liu P. F., Zhao C. S., Gobel T., Hallbauer E., Nowak A., Ran L., Xu W. Y., Deng Z. Z., Ma N., Mildenberger K., Henning S., Stratmann F., and Wiedensohler A. (2011) Hygroscopic proper ties of aerosol par ticles at high relative humidity and their diurnal variations in the Nor th China Plain, Atmos. Chem. Phys. Discuss., 11, 2991–3040

[38] Penner, J.E., et al., (1994). Quantifying and minimizing uncertainty of climate forcing by anthropogenic aerosols. Bulletin of the American Meteorological Society 75, 375–400.

[39] IPCC, (2001). Climate Change 2001, The Scientific Basis. Cam-bridge University Press, Cambridge, UK (881pp).

[40] Carrico, C.M., Kus, P., Rood, M.J., Quinn, P.K., Bates, T.S., (2003). Mixtures of pollution, dust, sea salt, and volcanic aerosol during ACE-Asia: radiative properties as a function of relative humidity. Journal of Geophysical Research 108 (D23), 8650.

[41] Kotchenruther, R.A., Hobbs, P.V., Hegg, D.A., (1999). Humidi-fication factors for atmospheric aerosol off the mid-Atlantic coast of the United States. Journal of Geophysical Research 1043, 2239–2251.

[42] Im, J.-S., Saxena, V.K., Wenny, B.N., (2001). An assessment of hygroscopic growth factors for aerosols in the surface boundary layer for computing direct radiative forcing. Journal of Geophysical research 106 (D17), 20213–20224.

[43] Hegg, D.A., Covert, D.S., Crahan, K., (2002). The dependence of aerosol light scattering on RH over the Pacific Ocean. Geophysical Research Letters 29 (8), 1219.

[44] Magi, B.I., Hobbs, P.V., (2003). Effects of humidity on aerosols in Southern Africa during the biomass burning season. Journal of Geophysical Research 108 (D13), 8495.

[45] MaXling, A., Wiedensohler, A., Busch, B., NeusuX, C., Quinn, P., Bates, T., Covert, D., (2003). Hygroscopic properties of different aerosol types over the Atlantic and Indian Oceans. Atmospheric Chemistry and Physics 3, 1377–1397.

[46] Maria, S.F., Russell, L.M., Gilles, M.K., Myneni, S.C.B., (2004). Organic aerosol growth mechanisms and their climate-forcing implications. Science 306, 1921–1924.

[47] White, W.H., Roberts, P.T., (1977). On the nature and origins of visibility-reducing aerosols in the Los Angeles air basin. Atmospheric Environment 11, 803–812.

[48] Tang, I.N., Wong, W.T., Munkelwitz, H.R., (1981). The relative importance of atmospheric sulfates and nitrates in visibility reduction. Atmospheric Environment 12, 2463–2471.

[49] Malm, W.C., Day, D.E., Kreidenweis, S.M., Collett, J.L., Lee, T., (2003). Humidity-dependent optical properties of fine particles during the big bend regional aerosol and visibility observational study. Journal of Geophysical Research 108 (D9), 4279.

[50] Doherty, et al., (2005). A comparison and summary of aerosol optical properties as observed in situ from aircraft, ship, and land during ACE-Asia. Journal of Geophysical Research 110, D04201.

[51] Gasso´ , S., et al. (2000), Influence of humidity on the aerosol scattering coefficient and its effect on the upwelling radiance during ACE-2, Tellus, Ser. B , 52, 546 – 567.

[52] Quinn, P. K., et. al. (2005) , Impact of particulat e organic matter on the relative humidity dependence of light scattering: A simplified parameterization, Geophys. Res. Lett., 32, L22809, doi:10.1029/2005GL024322.

[53] Clarke, A., et al. (2007), Biomass burning and pollution aerosol over North America: Organic components an d their influence on spectral optical properties and humidification response, J. Geophys. Res., 11 2, D12S18, doi:10.1029/2006JD007777.

[54] Fitzgerald, J. W. (1975) Approximation formulas for the equilibrium size of an aerosol particle as a function of its dry size and composition and ambient relative humidity. J. Appl. Meteorol., 14, 1044 –1049

[55] Tang, I. N. (1996) Chemical and size effects of hygroscopic aerosols on light scattering coeffcients. J. Geophys . R es. , 101, 19245 – 19250